Automatic Liver Segmentation
in Contrast-enhanced MRI

René Siewert[1], Dirk Schnapauff[2], Timm Denecke[2], Thomas Tolxdorff[1],
Dagmar Krefting[1]

[1]Institut für Medizinische Informatik, Charité–Universitätsmedizin Berlin
[2]Institut für Radiologie, Charité–Universitätsmedizin Berlin
`rene.siewert@charite.de`

Abstract. A fully automated method for liver segmentation in contrast enhanced abdominal MRI scans is presented. Liver shape and volume are obtained utilizing a context based approach. Compared to manual segmentation, the obtained liver volumes differ less than 10 %. The mean sensitivity of 0.92 is comparable to other published liver segmentation methods.

1 Introduction

Image based analysis of a patient's or a potential transplant donator's liver is vital for diagnosis, therapy and treatment control; and liver segmentation is an active research area. Anyhow, due to the high number of liver shape variants, and the wide range of morphological and structural changes due to liver-affecting disorders and diseases, robust liver segmentation is still a challenging task. Most algorithms are developed for CT-scans as the current goldstandard for liver imaging[1, 2]. In order to reduce the patient's X-ray exposure, efforts are notable to at least partially replace CT-scans by MRI. These efforts are supported in particular by new MRI contast agents. The specific contrast agent Gd-EOB (Primovist® in Europe or Eovist® in the U.S.) allows for MRI based lesion detection and characterization[3] and is a promising alternative for presurgical abdominal scans. As the exact measurement of the liver volume is required for therapy planning, these scans are currently segmented manually using the software provided by the manufacturer of the scanner, as existing liver segmentation algorithms developed for CT are not applicable for MRI. This is due to the fact, that intensity ranges and distribution in MRI differ strongly from CTs. Furthermore the image contrasts change with the use of contrast agents, so even MRI specific liver segmentation algorithms could not be applied to our data [4, 5, 6]. Therefore, we have developed a fully automated liver segmentation method for Primovist® enhanced abdominal MRI. A context based approach has been chosen for the segmentation algorithm. The basic idea of context based segmentation is the classification of image areas by subsequently applying a set of predefined rules to the image. These rules are strongly related to the human decisions taken during the respective pattern or object recognition task, and try

to comprise the experts knowledge. Each rule creates a dependency between different classes of the image. These dependencies form the image context. After all rules are applied, the image context should represent a valid segmentation. The main task within this approach is the formulation of a robust set of rules. In practice, a rule compares different features between image objects. Typical features are intensity or shape/size related, as well as comparative features between objects, such as relative location, distance or intensity difference. In order to get a robust initial segmentation, the basic rules are often formulated in the way to avoid false positives, resulting in an incomplete segmentation. Following the assumption, that possible „false negatives"(FN) are in the vicinity of the found segmentation and show certain similarities to the neighboring „true positives"(TP), morphological operations have proved to be a good choice to complete the segmentation.

2   Methods

In total, ten abdominal contrast enhanced MRI scans (*GE Signa Excite*, 3d-T1w fat saturated (LAVA) sequences, single breath-hold acquisition, 2 mm slice thickness) of the liver in the hepatobiliary phase (20 minutes after administration), have been taken within the clinical routine. Primovist is specifically uptaken by liver parenchyma (hepatocytes), thus brightening healthy liver tissue in T1-weighted MRI (parenchymal enhancement). Hepatic vessels and lesions with no or minimal hepatocytic function (cysts, metastases, the majority of hepatocellular carcinomas) will remain unenhanced and appear as dark objects within the liver region. Anyhow, the intensity of healthy liver tissue show gradients, appearing darker in the center of the liver, additionally to an overall gradient in B-field direction, often found in MRI. The grey-value range of the liver parenchyma overlaps with other organs, like kidneys, structures of the abdominal wall or sometimes the stomach even in the same slice (Fig. 1).

   Due to the high variety of liver shapes, mainly intensity based features are employed, especially strong edges found at the liver boundary; complemented by spatial and local shape information. As the overall intensity gradient in B-Field direction is significant, many features are extracted for each slice separately,
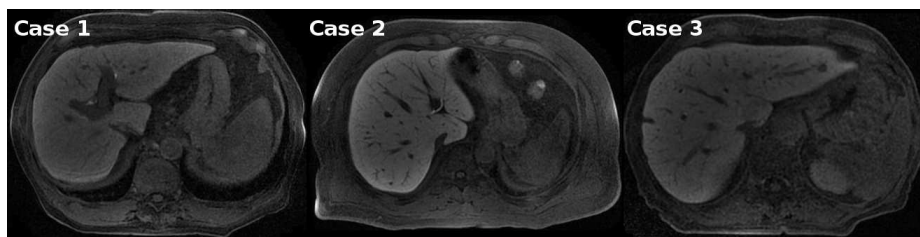

Fig. 1. Contrast enhanced MRT of the liver, different liver shapes.

combining the resulting classes to 3D objects occasionally. The algorithm scheme can be devided into seven steps:

1. Generous intensity based edge detection
2. Knowledge based elimination of false positive liver edges
3. Detection of strong edge and adjacent bright object pairs (liver seeds)
4. Initial liver segmentation
5. Morphological region growing of liver seeds
6. 3D-Reconstruction of found liver
7. Intensity based smoothing of the liver shape

For each slice $(S_{i,o})$, a median filtered $(S_{i,m})$ and a subsequently Sobel filtered derivative $(S_{i,s})$ are generated. Both filter methods use a $3{\times}3$ rectangular filter kernel. Edge detection (Step 1) is performed by histogram based thresholding of $S_{i,s}$. The threshold T_1 is found by $T_1 = \mathrm{mean}(P_{95}){+}2/3\sigma(P_{95})$, where P_{95} is the 95 percentile of $S_{i,s}$ and σ denotes the standard deviation. In the subsequent Step 2, false positives of the detected boundary objects are eliminated by evaluation of the position. The pixels belonging to the liver are assumed to be located mainly in the upper-left part of the slices. Therefore objects with the center of mass being found in the lower right quadrant of the slice are excluded. Then bright objects, defined by objects being above threshold $T_2 = \mathrm{mean}(S_{i,m}) + 2/3\sigma(S_{i,m})$, that are connected to the found liver border, are identified as liver parts (Step 3). If no bright objects are found along a particular border, the border itself is excluded from the liver border class. The initial (incomplete) liver segmentation is obtained by taking the largest connected component found in 3D reconstruction of the found 2D liver objects (Step 4). The missing liver parenchyma (Step 5) is now found by again slice based region growing processes of the liver parts. The evaluation of the growing criteria is performed on a further filtered derivative of the MRI scan $S_{i,nb} = 1/2(S_{i,o} + S_{i,m}) - S_{i,s}$. Within this combined image, the overall intensity is slightly smoothed, but strong edges appear as dark borders, and prohibit leakage of the liver parts across the border during the region growing process. The alternative stop criteria for the region growing are given by:

– The candidate pixel's intensity is lower than $\mathrm{mean}(S_{i,nb})$
– The candidate pixel's intensity is lower than the intensity of the respective seed pixel (5 % tolerance is considered),
– More than 1/3 of the pixels within the range 4 Moore neighborhood of the candidate pixel are already belonging to the liver object.

The resulting liver volume is again reconstructed from the found 2D-liver objects (Step 6), and the shape is smoothed by morphological opening with a diamond shaped structuring element of range 3 (Step 7).
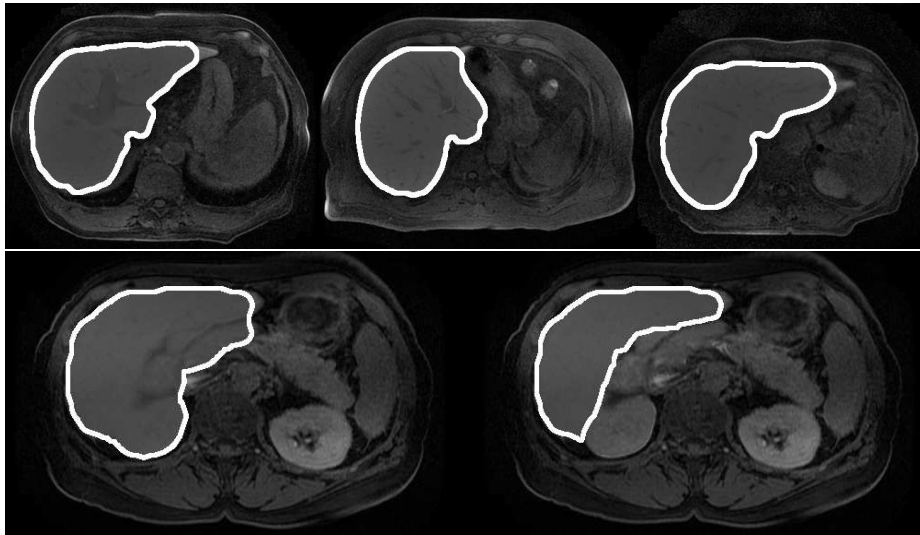
3   Results

The proposed method is applied to ten clinical datasets of healthy patients as well as patients suffering from liver cancer. The results obtained are compared to manual segmentation provided by the attending radiologist. As

Table 1. Segmentation results. aVol = automatic Volume; mVol = manual Volume.

Case	1	2	3	4	5	6	7	8	9	10	mean	σ
mVol[ml]	1671	1750	1380	1904	1626	1026	1341	1427	1377	2666		
aVol [ml]	1601	1647	1345	1779	1718	1085	1212	1417	1405	2665		
ΔVol[%]	-4,18	-5,90	-2,53	-6,59	+5,64	+5,73	-9,61	-0,68	+2,04	-0,06	$\pm$4,2	3,0
Sens	0,931	0,914	0,924	0,900	0,949	0,930	0,854	0,940	0,953	0,934	0,92	0,041

quality measures, the deviation ΔVol of the automatically obtained liver volumes (aVol) to the manual result (mVol), as well as the pixel-wise sensitivity $\text{Sens} = TP/(TP+FN)$, are chosen. The results are given in Tab. 1; Fig. 2 show exemplary segmentation results.

The measured liver volumes span the wide range of $\text{Vol}_{\min} = 1026\,\text{ml}$ to $\text{Vol}_{\max} = 2666\,\text{ml}$. All deviations in liver volumetry are within an acceptable tolerance of 10 %. The mean Volume error is $\text{mean}(\Delta\text{Vol}) = \pm 4.2\,\%$ with $\sigma(\Delta\text{Vol}) = 3,0\,\%$. The mean sensitivity is found to be $\text{mean}(\text{Sens}) = 0.92$ with $\sigma(\text{Sens}) = 0,041$. These results are comparable to those found for published segmentation methods, e.g. $\text{Sens} = 0.92$ [7], $\text{Sens} = 0.96$ and $\Delta\text{Vol} = 3\,\%$ [8] for CT segmentation. For the two reported fully automatic MRI based liver segmentation methods, no comparable measures are availabe. Massoptier et al. give a mean sensitivity $\text{Sens} = 0.95$ for ten datasets encompassing CT and MRI scans [6], while Logeswaran et al. do not give any quantitative measures at all [4]. The obtained results are promising, however, a critical point within the

Fig. 2. Segmentation results for different liver shapes (top) inaccurate result including kidney (bottom left), and corresponding manual segmentation (bottom right).

segmentation turned out to be the correct exclusion of the right kidney. In fact the right kidney may be closely attached to the liver, and show similar intensity values. An example is given in the bottom row of Fig. 2).

4   Conclusion

The proposed segmentation method is a promising approach for liver segmentation of contrast enhanced liver MRI. It is capable of segmenting liver organs with atypical shape as shown in cases from clinical routine. To date, it remains a tendency towards underestimation of the volume, and in few cases inclusion of the kidney into the segmentated area is observed. Further evaluation with more cases and different MRI scanner manufacturers are envisioned to enhance robustness and accuracy.

References

1. Campadelli P, Casiraghi E, Esposito A. Liver segmentation from computed tomography scans: Asurvey and a new algorithm. Artif Intell Med. 2009;45:185–96.
2. Heimann T, van Ginneken B, Styner MA, et al. Comparison and evaluation of methods for liver segmentation from CT datasets. IEEE Trans Med Imaging. 2009 Aug;28:1251–65.
3. Huppertz A, Balzer T, Blakeborough A, et al. Improved detection of focal liver lesions at mr imaging: multicenter comparison of gadoxetic acid enhanced mr images with intraoperative findings. Radiol. 2004;230:266–75.
4. Logeswaran R, Haw TW, Sarker SZ. Liver isolation in abdominal MRI. J Med Syst. 2008;32:259–68.
5. Platero C, González P, Tobar MC, et al. Automatic method to segment the liver on multi-phase MRI. In: CARS; 2008.
6. Massoptier L, Casciaro S. Fully automatic liver segmentation through graph-cut technique. Proc IEEE Eng Med Biol Soc. 2007;2007:5243–6.
7. Park H, Bland P, Meyer C. Construction of an abdominal probabilistic atlas and its application in segmentation. IEEE Trans Med Imaging. 2003;22(4):483–92.
8. Lim SJ, Joeng YY, Ho YS. Segmentation of the liver using deformable contour method on CT images. Lect Notes Computer Sci. 2004;3767:570–81.